Displacement of domain walls under a nanocontact current: Mechanism for magnetoresistance asymmetric switching

V. V. Osipov,[a] E. V. Ponizovskaya, and N. García
Laboratorio de Física de Sistemas Pequeños y Nanotecnología, C.S.I.C., c/Serrano 144, 28006 Madrid, Spain

(Received 8 March 2001; accepted for publication 16 July 2001)

We study the action of a magnetic field induced by nanocontact current pulses on the domain walls in thin magnetic films. We show that the pulses of a certain current direction shift the wall to the contact. Such an effect of attraction of the wall to the nanocontact does not depend on the initial position of the wall relative to the contact and results in an increase of nanocontact magnetoresistance. The opposite pulses repel this wall from the contact, i.e., the field action depends on the current direction. Our calculations explain experimental data relating to magnetoresistance devices. © *2001 American Institute of Physics.* [DOI: 10.1063/1.1403315]

In Refs. 1–3, it has been reported that magnetoresistance variations of ballistic Ni nanocontacts can exceed 700% at room temperature. The authors of Refs. 2 and 3 observed switching of the nanocontact resistance and an increase of the magnetoresistance under nanocontact current pulses. They assumed that these effects are due to reconstruction of the local magnetization configuration. Spin-injection switching of the magnetization direction by an electrical current has been predicted in Ref. 4. Displacement of the Bloch wall induced by a current parallel to the film plane was studied in Ref. 5. However, in the experiment,[2,3] the current flows normal to the film plane through a contact generating a radially symmetrical field (Fig. 1) which decreases as $1/r$ outside the contact. The effect of such a field induced by short pulses of an electron beam on homogeneous magnetic state in films was studied in Ref. 6.

In this letter, we study the action of nanocontact current pulses on the conventional Neel wall [Figs. 1(a)–1(c)] and ''head-to head'' structure [Figs. 1(d)–1(e)] in thin films. We show that the Neel wall situated to the left-hand side or to the right-hand side of the contact shifts to it under the pulses of the same current direction and repels from it under the opposite pulses. These effects arise from the asymmetric interaction between the magnetic field **H** induced by the nanocontact current and the magnetization **M** in the wall: it rotates **M** from the initial state [solid arrows in Fig. 1(b)] to the final state (dotted arrows) and shifts the wall towards the contact (from the point 0 to 0′). The interaction between **H** and **M** in the head-to-head wall is different and it is maximum when the contact is situated at the wall center [Fig. 1(e)].

We consider a thin uniaxial ferromagnetic film in which the easy axis lies in the film plane and the energy density of magnetic structures is[7–9]

$$w = A\{(\nabla\theta)^2 + \sin^2\theta[(\nabla\phi)^2]\} + K\sin^2\theta - \mathbf{M}\cdot\mathbf{H} - 1/2\mathbf{M}\cdot\mathbf{H}_d, \quad (1)$$

where θ is the angle between the easy axis x and the magnetization **M**; ϕ is the angle between the projection of **M** onto the plane (y and z) and the z axis [Fig. 1(a)]; A and K are the coefficients of exchange interaction and anisotropy; $\nabla = \mathbf{i}\partial/\partial x + \mathbf{j}\partial/\partial y$; $\mathbf{H}_d$ is the demagnetizing field. Here **H** is the external magnetic field induced by a current I along a nanowire of radius r_0. $H = I/2\pi r$ where $I = J\pi r^2$ at $r \leqslant r_0$ and $I = J\pi r_0^2 = I_0$ at $r > r_0$. $\mathbf{M}\cdot\mathbf{H} = -M_s H(\cos\varphi\sin\theta\sin\phi - \sin\varphi\cos\theta)$ where r and φ are shown in Fig. 1(a). In the thin films, Neel-wall domain structures arise.[8,9] The energy of the demagnetizing field of the Neel wall is a negligible component of its energy.[8] So we assume that $\mathbf{H}_d = H_z = -4\pi M_z = -4\pi M_s\sin\theta\cos\phi$ and $\mathbf{M}\cdot\mathbf{H}_d = -4\pi M_z^2 = -4\pi M_s^2\sin^2\theta\cos^2\phi$.

Using Eq. (1) the Landau–Lifshitz equation[7] can be written as

$$\partial\theta/\partial t = \alpha^{-1}F_\phi\sin\theta + F_\theta,$$
$$\partial\phi/\partial t\sin\theta = F_\phi\sin\theta - \alpha^{-1}F_\theta, \quad (2)$$

$$F_\theta = 2\nabla^2\theta - \sin 2\theta(\nabla\phi)^2 - \sin 2\theta + \partial h/\partial\theta - h_s\sin 2\theta\cos^2\phi, \quad (3)$$

$$F_\phi = 2\sin^2\theta\nabla^2\phi + 2\sin 2\theta(\nabla\phi\nabla\theta) + \partial h/\partial\phi + h_s\sin^2\theta\sin 2\theta, \quad (4)$$

where γ is the gyromagnetic ratio and α is the Gilbert parameter for viscous damping, $h_s = 2\pi M_s^2/K$ and $h = h(r)\times(\cos\varphi\sin\theta\sin\phi - \sin\varphi\cos\theta)$ where $h(r) = h_0 H(r)/H(L)$ and $h_0 = M_s H(L)/K$. The units of time and length are $t_0 = (1+\alpha^2)M/\alpha\gamma K$ and $L = (A/K)^{1/2}$; $t_0 \simeq (20-100)$ ps for typical parameters of Ni and Co. We assume that $\delta\mathbf{M}/\delta\mathbf{n} = 0$ on the sample boundaries where **n** is normal to the surface (see also below).

Figure 2 shows the dynamics of the wall situated at the initial moment [Fig. 2(a)] to the right-hand side of the contact, which is at the central point ⊕ where $x = y = 40$. Numerical analysis is carried out on the net 80×80 with the integration steps $\Delta t = 10^{-5}$ and $\Delta x = 0, 15$, i.e., for a sample size $12L\times12L$. The wall shape in the section is close to the well-known structure $\tan\theta/2 = \exp(x - x_0)$ with $x_0 = 50$ and $\theta(40,40) = \theta_0 = 0.44$ at the point ⊕. Under the action of the

[a]Electronic mail: osipov@fsp.csic.es

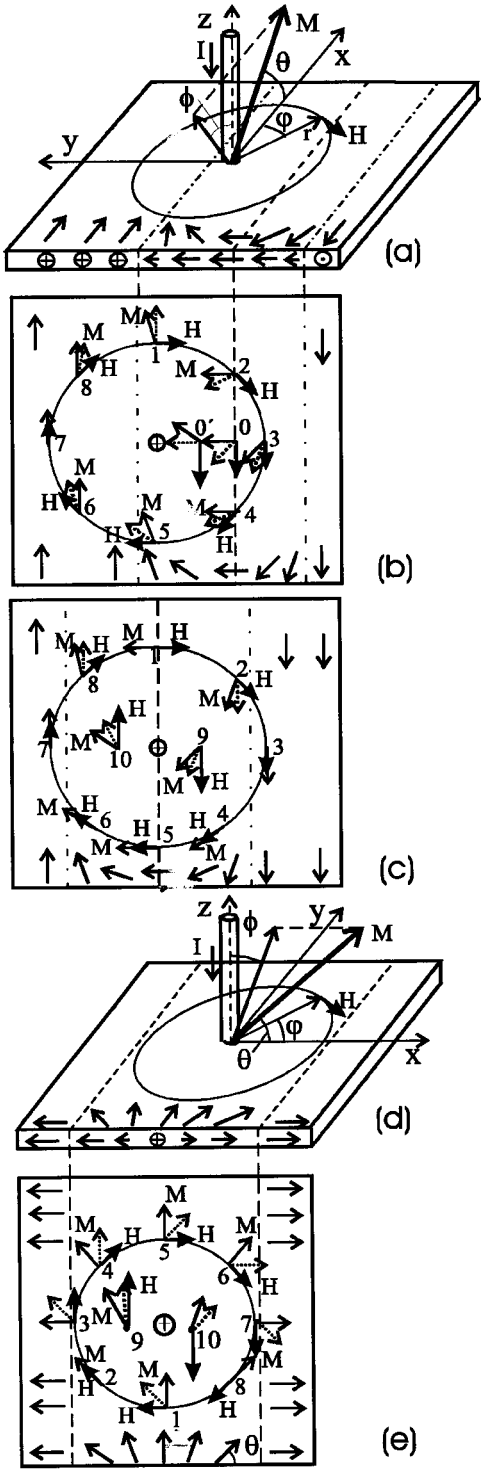

FIG. 1. Schematic representation of a thin magnetic film near the nanocontact (a) and of the configurations of the magnetization **M** in the Neel domain walls and of the magnetic field **H** induced by the nanocontact current **I**: (b) for a conventional wall situated to the right-hand side of the contact, (c) when the center line (dotted line) of the wall crosses the contact, (d) and (e) the same for a head-to head wall structure are shown. The dashed lines show the wall boundaries at the initial moment. The solid and dotted arrows show the initial and final states of **M**, respectively.

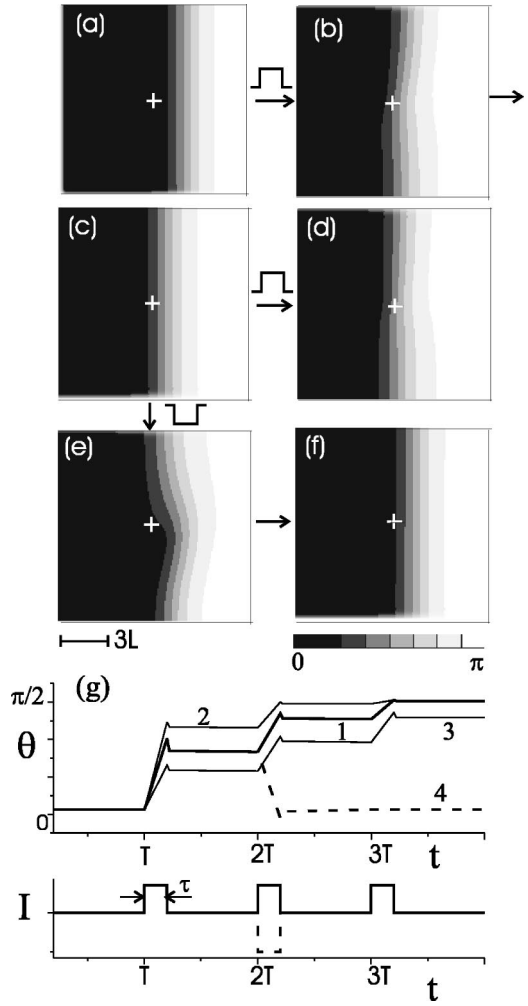

FIG. 2. Dynamics of the Neel wall under the action of nanocontact current pulses. Results of the numerical analysis of Eqs. (2)–(4) for a sample of size $12L\times 12L$, $r_0/L=0.5$ and $\alpha=1$: (a) initial state is a wall situated to the right-hand side of the contact, (b) state after the first pulse of amplitude $h_0=0.7$ and duration $\tau=5t_0$, (c) stationary state at $t=T=50t_0$, (d) state after a second pulse of the same amplitude at time $t=2T+\tau$, (e) state after a reverse pulse of amplitude $h_0=-1$ and duration $\tau=5t_0$, (f) stationary state after a reverse pulse at the time $t=2T+\tau$, and (g) variations of the angle $\theta=\theta_0$ at the nanocontact point under the action of series of the pulses are shown. White and black domains correspond to $\theta=\pi$ and $\theta=0$, respectively.

current pulse, the wall is distorted and moves to the left-hand side [Fig. 2(b)]. A stationary state with $\theta_0=1$, 18 is formed when the pulse duration $\tau\geqslant 5t_0$. After the pulse, the wall straightens and goes to another stationary form with $\theta_0=1.04$ and $x_0=44$ for time $T>20t_0$ [Fig. 2(c)]. The wall shifts to $\theta_0=1.38$ and $x_0=42$ after the second pulse [Fig. 2(d)], to $\theta_0=1.54$ and $x_0=41$ after the third pulse, and then it responds weakly to the next pulses. The corresponding changes $\theta(t)$ are shown in Fig. 2(g) (curve 1). When we increase the parameters h_0 and τ, the function $\theta(t)$ varies as curve 2, and when we decrease them $\theta(t)$ varies as curve 3 in Fig. 2(g). When $h_0\leqslant h_c=0.1$, the wall is deformed very little by the pulses and retains its original state. The greater the value of x_0, the higher h_c, i.e., the threshold current of the wall shift. All these results depend little on the boundary conditions and the value of α. However, the smaller the value of α, the longer the real pulse duration $\tau=5t_0$ as $t_0\propto\alpha^{-1}$ and the higher the threshold h_c.

When the contact is at the wall center, the upper part of the wall, $x>0$, is constricted but the wall remains at the point $\oplus$ under the action of current pulses of any directions. It follows from the interaction between **H** and **M**: **H** is practically parallel to **M** at the lower points 3–7 while the directions of **H** and **M** differ essentially at the upper points 1, 2,

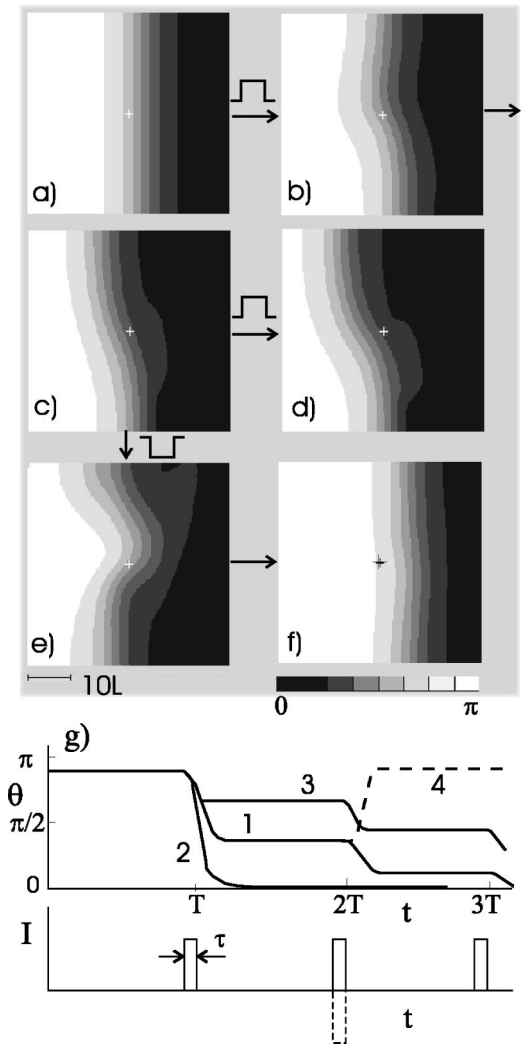

FIG. 3. The same as in Fig. 2 but for a head-to-head Neel-wall structure.

and 8 in Fig. 1(c). However, if after the first pulse [Fig. 2(c)] we apply an opposite pulse with $-h_0 \geqslant 0.7$, the wall is deformed in the opposite manner [Fig. 2(e)] and shifts to the original state or to its right-hand side [Fig. 2(f) and dotted curves in Fig. 2(g)].

The results of our calculations agree in detail with the main experimental data reported in Refs. 2 and 3. Indeed, let us suggest that the magnetization within the nanocontact is directed along the axis *y* and so its resistance is large enough and the magnetoresistance is very small when domain walls are far away from the contact. Under the action of current pulses of any direction, one of the nearest walls will move to the nanocontact and is fixed near it. As a result, the nanocontact resistance decreases, as **M** in the wall center is also directed along the axis *y* [Fig. 1(a)], and the magnetoresistance increases due to the displacement of the wall under the external magnetic field. The magnetoresistance variations depend little on direction of the field. These effects are actually observed in the experiment. In particular, the form of the curves presented in Fig. 3(g) coincides with that of the experimental curves.[2,3] The experimental pulse duration $\tau \simeq 100\,\mathrm{ns} \gg 5t_0$ and so small spikes found in our calculations after the pulses [see Fig. 3(g)] could not be observed in the experiment. Moreover, the value $h_0 = 0.7$ corresponds approximately to the current $I \simeq 70\,\mathrm{mA}$ which was used in the experiment.

We also studied the dynamics of the head-to-head Neel wall [Fig. 1(d) and (e)] and found that such wall is shifted by the same current pulses but it is distorted in a different manner (Fig. 3). Its displacement is maximum when the contact is situated at wall center and the direction of the displacement depends on the current direction. Under the action of the current pulse, the wall situated to the right-hand side of the contact with $\theta_0 = 2.7$ [Fig. 3(a)] is distorted and moves to the left-hand side [Fig. 3(b)] where $\theta_0 = 1.9$. After the pulse, the motion of the curved wall continues, the wall straightens and goes to another stationary form with $\theta_0 = 0.97$ for time $T > 20t_0$ [Fig. 3(c)]. The wall shifts to $\theta_0 = 0.3$ after the second pulse [Fig. 3(d)], to $\theta_0 = 0.1$ after the third pulse, and then it responds little to the next pulses [curve 1 in Fig. 3(g)]. When a pulse of opposite polarity is applied, following the first pulse [Fig. 3(c)], with $-h_0 \geqslant 0.7$, the wall is deformed on the opposite manner [Fig. 3(e)] and then it shifts to the original state or to the right of it [Fig. 3(f) and dotted curves in Fig. 3(g)]. When the parameters h_0 and τ increase or decrease the function $\theta(t)$ varies as curve 2 or curve 3 in Fig. 3(g), respectively.

Thus, we have calculated the displacement of the domain walls in thin films under the action of nanocontact current pulses and found: (i) The motion of the wall depends on its structure, (ii) The wall displacement and therefore the magnetoresistive effect depend on the *direction of the current*, and (iii) These effects occur without a spin-polarized current and are determined only by the electrodynamics.

Finally, in view of the asymmetric action of the induced field depending on the current direction, one may consider the interpretation of recent experiments[10] taking into account the theory developed here. This work is now in progress.

This work has been supported by EU Contract No. IST-2000-26011. One of the authors (V.V.O) was supported by the Spanish Sabbatical Program and another author (E.V.P.) by the NATO Science Program. The authors thank Professor J. A. Rausell Colom and Dr. I. G. Saveliev for helpful remarks.

[1] N. Garcia, M. Muñoz, and Y.-W. Zhao, Phys. Rev. Lett. **82**, 2923 (1999); G. Tatara, Y.-W. Zhao, M. Muñoz, and N. Garcia, Phys. Rev. Lett. **83**, 2030 (1999).
[2] N. Garcia, I. G. Saveliev, Y.-W. Zhao, and A. Zlatkine, J. Magn. Magn. Mater. **214**, 7 (2000).
[3] N. Garcia, H. Rohrer, I. G. Saveliev, and Y.-W. Zhao, Phys. Rev. Lett. **85**, 3053 (2000); Recent unpublished work on ballistic magnetoresitance in electrodeposited nanocontacts shows magnetoresitace up to 700%.
[4] J. C. Slonczewski, J. Magn. Magn. Mater. **159**, L1 (1996); *ibid.***195**, L261 (1999); L. Berger, Phys. Rev. B **54**, 9353 (1996).
[5] L. Berger, Phys. Chem. Solids **35**, 947 (1974); E. Salhi and L. Berger, J. Appl. Phys. **76**, 4787 (1994); C.-Y. Hung and L. Berger, J. Appl. Phys. **63**, 4276 (1988); L. Berger, J. Appl. Phys. **69**, 1550 (1991).
[6] C. H. Back, R. Allenspach, W. Weber, S. S. P. Parkin, D. Weller, E. L. Garwin, and H. C. Siegmann, Science **285**, 864 (1999).
[7] A. P. Malozemoff and J. C. Slonczewski, *Magnetic Domain Walls in Bubble Materials* (Academic, New York, 1979).
[8] A. Aharoni, *Introduction to the Theory of Ferromagnetism* (Oxford University Press, New York, 1998).
[9] A. Hubert and R. Schafer, *Magnetic Domains* (Springer, Berlin, 1998).
[10] J. A. Katine, F. J. Albert, R. A. Buhrman, E. B. Myers, and D. C. Ralph, Phys. Rev. Lett. **84**, 3149 (2000).